

LBL-28013  
ESG Note-81

## Flip-Flop Modes in Symmetric and Asymmetric Colliding-Beam Storage Rings\*

J. L. Tennyson

Accelerator and Fusion Research Division  
Exploratory Studies Group  
Lawrence Berkeley Laboratory  
1 Cyclotron Road  
Berkeley, CA 94720

August 1989

\* This work was supported by the Director, Office of Energy Research, Office of High Energy and Nuclear Physics, High Energy Physics Division, of the U.S. Department of Energy under Contract No. DE-AC03-76SF00098.

# Flip-Flop Modes in Symmetric and Asymmetric Colliding-Beam Storage Rings

*J. L. Tennyson*

*Lawrence Berkeley Laboratory, MS 71-259, Berkeley CA 94720*

## ABSTRACT

A model of self-consistent beam blow-up in a colliding beam storage ring is described which explains the appearance of flip-flop modes in both symmetric and asymmetric beam systems. It derives the strong-strong steady-states and their stabilities from the weak-strong behavior. This model agrees well with the observed flip-flop behavior in storage rings, including the hysteresis seen when the beams are flipped from one asymmetric steady state to the other. It can be used to predict the behavior of proposed facilities in which the two colliding beams are characterized by different parameters.

## 1. Introduction

The luminosities of many colliding-beam storage rings are limited by the beam-beam interaction, the relativistically enhanced transverse electromagnetic force that a particle of one beam sees as it passes through a bunch of the opposing beam. The beam-beam interaction can cause transverse blowups of the two beams and/or shortening of beam lifetime. Studies of the beam-beam interaction have generally fallen into one of two general groups: weak-strong studies and strong-strong studies.

The weak-strong model of the beam-beam interaction assumes that the interaction is one-way; that beam #1 affects beam #2 but not vice versa. This allows one to study the nonlinear behavior of the system without the added complexity of self-consistency. The strong-strong model, which in most cases is more realistic, assumes that beam #1 affects beam #2 and is simultaneously affected by beam #2. Unlike weak-strong equilibria, strong-strong equilibria may be time-dependent; they may either oscillate regularly in time (a limit cycle) or evolve chaotically (a chaotic attractor). The strong-strong model, because it requires that the behaviors of the two beams be self-consistent, is typically more complicated and more difficult to understand than the weak-strong.

It is shown here that, under certain conditions, strong-strong behavior can be determined from weak-strong behavior. These conditions are 1) that the strong-strong steady-states be time-independent, and 2) that the RMS size of each beam depends only the spatial distribution of the opposing beam via its RMS width. These conditions are almost universally met in modern simulation models and there is evidence that they are nearly met in real machines.

That strong-strong time-independent equilibria can be studied with a weak-strong model is, to a certain extent, intuitively reasonable. The idea has been implicit in most of the weak-strong studies performed during the past fifteen years. An approach similar to the one presented here was used to construct a model of flip-flop phenomena at VEPP-2M and PETRA [1]. Certain elements of this analysis, the bifurcation in particular, play prominent roles in [2] and later studies by the same author.

The ability to derive strong-strong behavior from weak-strong behavior is advantageous in both theoretical and simulation studies. On a theoretical level, it allows one to concentrate on the relatively simple problem of explaining the statistical behavior of one beam when it collides repeatedly with an opposing beam of known fixed shape. On the simulation level, it allows one to productively study beam-beam effects with the more time efficient weak-strong algorithms, and to check the behaviors of strong-strong algorithms by comparing them to the behaviors theoretically predicted from the weak-strong results.

Although the weak-strong theory of the beam-beam interaction is inherently simpler than the strong-strong, it is still far from complete. It is not yet sufficiently developed to predict, for example, the average luminosity of a proposed machine. This is because the beam-beam system is characterized by a "near-integrable" dynamic, a particularly intractable equation of motion exhibiting neither dynamical invariants (first integrals) nor statistical invariants (entropies). The nonlinearity destroys any potentially useful dynamical invariants while the KAM theorem frustrates statistically coherent behavior. Beam-beam kicks are correlated over very long periods of time and the decay rates of these correlations are extremely difficult to calculate. Statistical models, such as that proposed in [2], underestimate beam stability since they ignore long term correlations. Integrable dynamical models, such as that proposed in [3], tend to overestimate stability since they ignore the chaotic component of the motion that comes from nonlinear resonances.

A self-consistent model of the beam-beam interaction is described in Section 2. Section 3 discusses the stabilities of the self-consistent equilibria. Section 4 shows that, under the conditions stated in Section 2, the self-consistent equilibria can be derived from weak-strong equilibria. It is shown in Section 5 that the stabilities of the self-consistent equilibria can also be derived from the weak-strong behavior. Illustrative examples are given in Section 6.

## 2. Self-Consistent Equilibria (Strong-Strong Model)

A relatively simple theory of self-consistent beam-beam equilibria may be constructed given the following two assumptions:

- A. The system's "steady-state" solutions are time-independent, i.e. they are not limit cycles or chaotic attractors. This is generally true in real accelerators when no coherent modes are

excited. It is usually less true in strong-strong simulations where super-particle discreteness results in significant fluctuations at equilibrium.

- B.** The time derivative of the RMS size of each beam, when the system is close to an equilibrium, depends on the shapes of the two beams only via their RMS widths. In most strong-strong simulations, the time evolution of one beam depends on the shape of its opposing beam only via its RMS width, but the dependence on its own shape (via radiation damping and quantum excitation) is generally more complicated. In real machines, even the dependence on the shape of the opposing beam is more complicated. However, this approximation may be sufficiently valid as long as the beam shapes are never too far from Gaussian.

Note that the second assumption is considerably weaker than the assumption that the beams are Gaussian at all times. The latter assumption would not be true since, at the beam-beam limit, the edges of the beam in the six dimensional phase space are irregular and the density of particles in the tails (at large amplitude) is considerably larger than Gaussian. In fact, if the distributions at equilibrium *were* known to within a small number of parameters (e.g. if they were known to be Gaussian), then the evolution of the distribution function could be numerically calculated in a low dimensional parameter space (this was attempted in [1]). The near-integrable nature of the system's dynamic virtually insures that this cannot be done.

In addition to the primary assumptions **A** and **B**, it is also assumed for convenience that the two beams are round;  $\sigma_1 = \sigma_{x1} = \sigma_{y1}$  and  $\sigma_2 = \sigma_{x2} = \sigma_{y2}$ . Under these assumptions, the equations of motion for beam size have the general form

$$\dot{\sigma}_1 = V(\sigma_1, \sigma_2; \mathbf{p}_1) \tag{1}$$

$$\dot{\sigma}_2 = V(\sigma_2, \sigma_1; \mathbf{p}_2)$$

where  $\mathbf{p}$  is the set of all known constants affecting beam size.

$$\mathbf{p}_1 = \{v_{x1}, v_{y1}, v_{z1}, \beta_{x1}, \beta_{y1}, \eta_{x1}, \eta_{y1}, \tau_1, \sigma_{01}, N_2, \dots, \text{etc.}\} \tag{2}$$

$$\mathbf{p}_2 = \{v_{x2}, v_{y2}, v_{z2}, \beta_{x2}, \beta_{y2}, \eta_{x2}, \eta_{y2}, \tau_2, \sigma_{02}, N_1, \dots, \text{etc.}\}$$

Note that the rate at which a beam changes size depends on the size of the opposing beam via the beam-beam interaction and on its own size via synchrotron radiation effects. The equations (1) define a vector field in the  $(\sigma_1, \sigma_2)$  plane. A schematic representation of a typical vector field is shown in figure 1. The flow lines shown in the figure lie parallel to the vectors defined by (1). The vector field is

generally characterized by one or more attractors, which we have assumed (in A) to be generically isolated points. If there's more than one attractor, there will also be "basin boundaries" separating them.

The equilibria of the vector field are defined by the conditions

$$\begin{aligned} V(\sigma_1, \sigma_2; p_1) &= 0 \\ V(\sigma_2, \sigma_1; p_2) &= 0 \end{aligned} \tag{3}$$

Each of these conditions corresponds to a curve in the  $(\sigma_1, \sigma_2)$  plane. The intersections of these curves give the equilibria. The equilibria curves for figure 1 are represented in figure 2 by thick lines. The curves intersect the flow lines where they are either vertical or horizontal.

### 3. Stability

To determine the stability of the equilibria defined by (3), the equations of motion (1) are linearized. In a sufficiently small neighborhood of an equilibrium, the equations of motion can be approximated by the linearization

$$\begin{bmatrix} \dot{\delta\sigma}_1 \\ \dot{\delta\sigma}_2 \end{bmatrix} = \begin{bmatrix} \frac{\partial V_1}{\partial \sigma_1} & \frac{\partial V_1}{\partial \sigma_2} \\ \frac{\partial V_2}{\partial \sigma_1} & \frac{\partial V_2}{\partial \sigma_2} \end{bmatrix} \begin{bmatrix} \delta\sigma_1 \\ \delta\sigma_2 \end{bmatrix} \tag{4}$$

where  $\delta\sigma_1 = \sigma_1 - \sigma_{eq1}$  is the displacement from the equilibrium size of beam #1. We have used the shorthand notation

$$\begin{aligned} V_1 &= V(\sigma_1, \sigma_2; p_1) \\ V_2 &= V(\sigma_2, \sigma_1; p_2) \end{aligned} \tag{5}$$

The stability of the equilibrium is determined by the eigenvalues  $\lambda_+$ ,  $\lambda_-$  of the matrix

$$\mathbf{M} = \begin{bmatrix} \frac{\partial V_1}{\partial \sigma_1} & \frac{\partial V_1}{\partial \sigma_2} \\ \frac{\partial V_2}{\partial \sigma_1} & \frac{\partial V_2}{\partial \sigma_2} \end{bmatrix} \tag{6}$$

$$\text{Let } q \equiv \text{Det } [M] = \lambda_+ \lambda_- = \frac{\partial V_1}{\partial \sigma_1} \frac{\partial V_2}{\partial \sigma_2} - \frac{\partial V_2}{\partial \sigma_1} \frac{\partial V_1}{\partial \sigma_2} \quad (7)$$

$$p \equiv \text{Tr } [M] = \lambda_+ + \lambda_- = \frac{\partial V_1}{\partial \sigma_1} + \frac{\partial V_2}{\partial \sigma_2} \quad (8)$$

The eigenvalues are then

$$\lambda_{\pm} = \frac{p \pm \sqrt{p^2 - 4q}}{2} \quad (9)$$

There are three generic types of equilibria (see figure 1)

1. The equilibrium is an unstable *saddle point* if  
 $q < 0$  ( $\lambda_+, \lambda_-$  are both real with opposite signs) (10)

2. The equilibrium is a *node* (non-oscillating attractor or repeller) if  
 $0 < q < p^2/4$  ( $\lambda_+, \lambda_-$  are both real with the same signs) (11)

The *node* is stable if  $p < 0$  (11a)

and unstable if  $p > 0$  (11b)

3. The equilibrium is a *focus* (oscillating attractor or repeller) if  
 $p^2/4 < q$  ( $\lambda_+, \lambda_-$  are complex and conjugate to one another) (12)

The *focus* is stable if  $p < 0$  (12a)

and unstable if  $p > 0$  (12b)

#### 4. Derivation of Self-Consistent Equilibria from Weak-Strong Model

The function  $V(\sigma_a, \sigma_b; p_a)$  is not known analytically. It's possible to determine it empirically from simulation, but because the parameter space  $\{p\}$  has such a high dimensionality, this determination is practical only in a small locality of a given point  $p$ . Furthermore, finding  $V(\sigma_a, \sigma_b; p_a)$  is unnecessary in many accelerator applications because strong-strong simulations give the stable equilibria directly.

But ignorance of  $V(\sigma_a, \sigma_b; p_a)$  does not itself preclude a theoretical understanding of self-consistent equilibria. In fact, the self-consistent aspect of the problem, under certain conditions, can be separated entirely from the problem of finding  $V(\sigma_a, \sigma_b; p_a)$ . In this sense, the theory of beam-beam equilibria

can be factored into two independent parts: an understanding of the weak-strong model (roughly equivalent to finding  $V(\sigma_a, \sigma_b; p_a)$ ), and a way of determining the self-consistent behavior from the weak-strong behavior.

It is shown here, given the assumptions A and B above, that the self-consistent equilibria and their stabilities can be derived from the weak-strong behavior. The self-consistent equations of motion correspond to two weak-strong systems; one for each beam.

$$\text{System \#1} \begin{cases} \dot{\sigma}_1 = V(\sigma_1, \sigma_2; p_1) \\ \dot{\sigma}_2 = 0 \end{cases} \quad (13)$$

$$\text{System \#2} \begin{cases} \dot{\sigma}_2 = V(\sigma_2, \sigma_1; p_2) \\ \dot{\sigma}_1 = 0 \end{cases} \quad (14)$$

In each weak-strong system, the size of the strong beam becomes a fixed parameter and the state space reduces to one dimension. As with the self-consistent system, the equilibria are given by the conditions

$$\begin{aligned} \dot{\sigma}_1 = 0 & \quad \text{system \#1} \\ \dot{\sigma}_2 = 0 & \quad \text{system \#2} \end{aligned} \quad (15)$$

If one knows the locations in the  $(\sigma_1, \sigma_2)$  plane of the equilibria of both weak-strong beam systems, one can find from them all of the self-consistent equilibria. This is because the conditions (15) define curves in the  $(\sigma_1, \sigma_2)$  plane that are identical to those defined by the conditions (3). The intersections of these weak-strong equilibria curves thus correspond to the self-consistent equilibria.

The stabilities of the weak-strong equilibria are determined by the derivatives of  $V$ . A weak-strong equilibrium for  $\sigma_1$  is stable if, at the equilibrium,

$$\frac{\partial V(\sigma_1, \sigma_2; p_1)}{\partial \sigma_1} < 0 \quad (16)$$

Likewise, an equilibrium for  $\sigma_2$  is stable if

$$\frac{\partial V(\sigma_2, \sigma_1; p_2)}{\partial \sigma_2} < 0 \quad (17)$$

The curves defined by (15) each correspond to a continuous set of weak-strong equilibria that are either stable or unstable.

## 5. Derivation of Self-Consistent Stability from the Weak-Strong Model

It was demonstrated above that the self-consistent equilibria can be found from the intersections of the weak-strong equilibria curves (15). Finding the stability characteristics of the self-consistent equilibria is not quite so easy. A curve of weak-strong equilibria is typically represented by a function  $S(\sigma; \mathbf{p})$ . With arguments  $(\sigma_2; \mathbf{p}_1)$ , this  $S$  is the equilibrium beam size  $\sigma_{eq1}$  of beam #1; with arguments  $(\sigma_1; \mathbf{p}_2)$ , it is the equilibrium size  $\sigma_{eq2}$  of beam #2.

$$\begin{aligned}\sigma_{eq1} &= S(\sigma_2; \mathbf{p}_1) \\ \sigma_{eq2} &= S(\sigma_1; \mathbf{p}_2)\end{aligned}\tag{18}$$

Equations (18) correspond to solving equations (3) for  $\sigma_1$  and  $\sigma_2$  respectively. As with  $V(\sigma_a, \sigma_b; \mathbf{p}_a)$ , it's convenient to use the shorthand notation

$$\begin{aligned}S_1 &\equiv S(\sigma_2; \mathbf{p}_1) \\ S_2 &\equiv S(\sigma_1; \mathbf{p}_2)\end{aligned}\tag{19}$$

The function  $S(\sigma; \mathbf{p})$  will be called the weak-beam size function (WBS). In almost all cases of practical interest, there is only one such function. It is single-valued, and the equilibria it represents are stable. Illustrative examples are shown in figures 3a and 3b for two round beams operating on the coupling resonance at different tunes. Both the weak and strong beam sizes are normalized to the natural size of the weak beam. From (16), (17), (5) and (8), this means that the diagonal elements of the matrix  $M$  are negative and  $p = \text{Tr}(M) < 0$ . Note from (10)-(12) that this does not determine the stability of the self-consistent equilibrium, but it does eliminate unstable nodes and unstable foci. Thus, if the self-consistent equilibrium is unstable, it must be a saddle point. Whether or not it's a saddle point can be determined from the derivatives of  $S(\sigma; \mathbf{p})$ . To see this, notice that  $S(\sigma_2; \mathbf{p}_1)$  describes the contour  $V(\sigma_1, \sigma_2; \mathbf{p}_1) = 0$  in the  $(\sigma_1, \sigma_2)$  plane. Thus, the derivative of  $V(\sigma_1, \sigma_2; \mathbf{p}_1)$  in the direction defined by the curve  $S(\sigma_2; \mathbf{p}_1)$  is zero

$$dS_1 \frac{\partial V_1}{\partial \sigma_1} - d\sigma_2 \frac{\partial V_1}{\partial \sigma_2} = 0\tag{20}$$

or

$$\frac{dS_1}{d\sigma_2} = \frac{\partial V_1}{\partial \sigma_2} / \frac{\partial V_1}{\partial \sigma_1}\tag{21}$$

Similarly, for beam #2

$$\frac{dS_2}{d\sigma_1} = \frac{\partial V_2}{\partial \sigma_1} / \frac{\partial V_2}{\partial \sigma_2} \quad (22)$$

Using (21) and (22), it's possible to calculate the sign of the determinant of M. If

$$\frac{dS_1}{d\sigma_2} \frac{dS_2}{d\sigma_1} < 1 \quad (23)$$

then, from (21) and (22)

$$\left( \frac{\partial V_1}{\partial \sigma_2} / \frac{\partial V_1}{\partial \sigma_1} \right) \left( \frac{\partial V_2}{\partial \sigma_1} / \frac{\partial V_2}{\partial \sigma_2} \right) < 1$$

Using the fact that (16) and (17) are satisfied, this can be written

$$\frac{\partial V_1}{\partial \sigma_1} \frac{\partial V_2}{\partial \sigma_2} - \frac{\partial V_1}{\partial \sigma_2} \frac{\partial V_2}{\partial \sigma_1} > 0 \quad (24)$$

so that

$$\text{Det}(M) > 0 \quad (25)$$

It can be shown by a similar argument that (25) does not hold when (23) is not satisfied. It was pointed out above that because  $\text{Tr}(M) < 0$ , the equilibrium must be stable when  $\text{Det}(M) > 0$  and unstable when  $\text{Det}(M) < 0$ . Thus (23) is a criterion for the stability of the self-consistent equilibrium. The criterion is valid as long as the weak-strong equilibria are both stable and the two assumptions A and B are accepted. Note that for a symmetric system, an equilibrium on the diagonal of the  $(\sigma_1, \sigma_2)$  plane has

$$\frac{dS}{d\sigma} \equiv \frac{dS_1}{d\sigma_2} = \frac{dS_2}{d\sigma_1} \quad (26)$$

and the stability criterion (23) reduces to

$$\left| \frac{dS}{d\sigma} \right| < 1 \quad (27)$$

It may seem odd that a self-consistent equilibrium can be unstable even when its associated weak-

strong equilibria are both stable (and that the self-consistent equilibrium can be stable even when one of the weak-strong equilibria is unstable). This paradoxical situation is illustrated in figures 4a and 4b for the two conditions mentioned. In figure 4a, the equilibrium is unstable, but the flow lines all point inward where they cross the horizontal and vertical intercepts of the equilibrium. This means that motion constrained to either intercept will always approach the equilibrium. In figure 4b, the equilibrium is a stable focus but the flow lines point outward where they cross the vertical intercept. Motion constrained to that intercept would thus be unstable.

The WBS function  $S(\sigma; \mathbf{p})$  is far easier to measure and to work with than the more complicated  $V(\sigma_a, \sigma_b; \mathbf{p}_a)$ . If the assumptions A and B are correct (or sufficiently correct), the self-consistent equilibria and their stabilities can be obtained from  $S(\sigma; \mathbf{p})$  using (18) and (23). Solving the mystery of beam-beam blow-up then reduces to understanding the function  $S(\sigma; \mathbf{p})$ . It is known that  $S(\sigma; \mathbf{p})$  generally decreases monotonically with  $\sigma$  for all values of the parameters  $\mathbf{p}$ , and that it probably has a maximum value at  $\sigma = 0$ , or at least at some  $\sigma \ll 1$ . However little is known about the dependence on the parameters  $\mathbf{p}$ . Both simulation and experiment have shown that stronger weak-beam damping decreases  $S(\sigma; \mathbf{p})$ , and that coupling between the synchrotron and betatron motions increase it. However the precise dependence is not known. Typical graphs of  $S(\sigma; \mathbf{p})$  are shown in figure 5 for a variety of strong beam currents. These graphs were obtained from a simulation model with moderate chromaticity (modulation of the betatron tune by the synchrotron motion). For a symmetric collider, the self-consistent beam size at each current value is represented by the intersection of the appropriate curve with the diagonal (shown as a thick line). Figure 5 suggests that symmetric balanced beams with these parameter values will blow up until the current reaches  $3I_Q$ . At this value, the slope of  $S(\sigma; \mathbf{p})$  on the diagonal reaches -1 and the symmetric steady state goes unstable. At larger currents, the beams fall into a 'flip-flop' condition.

## 5. Examples

It is helpful to consider some hypothetical examples. In the first example, the two beams are symmetric. This is the usual condition in an electron-positron collider where two beams of equal current circulate in opposite directions in the same ring. Figure 6 shows a low current situation (representative, not actual) where the beam blow-up is insignificant. The two curves are graphs of the functions  $S_1$  and  $S_2$ . Their intersections, at  $\sigma_1=1, \sigma_2=1$ , give the self-consistent equilibrium. Note that the stability criterion (27) is satisfied at this point. As the currents in both beams are increased, the equilibrium begins to move out the diagonal, indicating that the beams are blowing up symmetrically (see figure 7). The crossing angle of the two curves decreases. The stability condition (27) continues to be met until the intersection of the two curves is no longer transverse. At this point, the slope of  $S$

on the diagonal is equal to -1. When the current exceeds this critical point, condition (27) is no longer fulfilled, and the equilibrium becomes a saddle point. Simultaneously, two stable satellite equilibria are born. These satellites correspond to the asymmetric “flip-flop” equilibria observed in many electron-positron colliders (e.g. SPEAR [4] and CESR [5]). The formation of the two satellite equilibria is an example of a “pitchfork bifurcation”. As the current is increased further, these equilibria rapidly move away from the diagonal (see figure 8).

A typical phase flow [6] for symmetric beams above the critical current is shown in figure 9. There are two basins of attraction. If the two beams are initially the same size, the system will first move approximately along the diagonal towards the saddle point. As it nears the saddle point, it will begin to veer to one side or the other, depending on fluctuations or a small initial imbalance. It will then fall into one or the other of the two point attractors. Whether these are nodes or oscillating foci depends on the magnitude of  $\text{Det}(M)$ . Just above the bifurcation, since  $\text{Det}(M)$  is still nearly zero, the stable equilibria will be nodes. However, it is theoretically possible for them to become foci as the current is increased further, pushing  $\text{Det}(M)$  above  $[\text{Tr}(M)]^2/4$  as shown in (12). The set of equilibria for all values of the current are plotted in figure 10. The familiar pitchfork shape is evident.

A beam system is called “asymmetric” if  $p_1 \neq p_2$ . Although some machines are theoretically symmetric, it’s rare that both beams are really identical. The lattice on either side of the IP may be subtly different, or the two beams might have slightly different currents. In other accelerators, this asymmetry may be an explicit design element. The “asymmetric” colliders now being considered for B-meson production are examples. The above analysis is not specific to symmetric configurations; in fact, it’s probably more useful in asymmetric applications because it provides an understanding of how the asymmetry affects the blow-up balance.

The flip-flop effect is so named because workers at SPEAR found that they could flip the beam system out of one stable asymmetric equilibrium and into the other by introducing an appropriate asymmetry in the lattice. This was done by varying the RF phasing in the cavities on either side of the IP. To see how an asymmetry can flip the system, consider an initially symmetric system above the critical point with beam #1 blown up and beam #2 close to its “natural” size, figure 11a. As the current in beam #2 is decreased, the parameter set  $p_1$  changes and the blow-up  $S_1$  also decreases. This causes the saddle point to approach the occupied stable equilibrium, as shown in figure 11b. When the current in beam #2 falls below a certain critical value, the saddle and stable equilibria meet and annihilate. The system then flips (figure 11c), falling into the opposite stable equilibrium with beam #2 blown up and beam #1 at its natural size. If the current in beam #2 is then restored to its initial value, the system remains in the new state. This type of hysteresis is characteristic of “cusp catastrophes” and is similar to the phenomena observed in a ferro-magnetic material when the polarity of the ambient magnetic field is reversed. A representative hysteresis curve for the flip-flop effect is shown in figure 12 where the difference between the two beam radii are plotted against the current in beam #2, assuming the current

in beam #1 remains fixed. Of course, the control parameter here need not be the current in beam #2. It could instead be any of several different parameters capable of significantly breaking the symmetry of the beam-beam system.

The pitch-fork bifurcation that occurs here is directly analogous to a second order phase transition. As with a phase transition, relaxation times become very long in the vicinity of the critical point. This is because one of the eigenvalues  $\lambda$  goes through zero at the critical point while the other is equal to the trace  $\text{Tr}(M)$ . For a symmetric system, the eigenvector corresponding to the small eigenvalue lies perpendicular to the diagonal while the non-zero eigenvector lies along the diagonal. Thus, a system just above the critical point and in a symmetric initial state  $(\sigma_1 - \sigma_2) = 0$  quickly approaches the saddle point. It then, very slowly, drifts away from the saddle toward one of the stable satellite equilibria. Additionally, if there is any noise in the system, the relatively weak stability of the satellite equilibria will result in a large response function for fluctuations perpendicular to the diagonal. This is a serious problem for strong-strong simulation programs where super-particle discreteness can drive large fluctuations in the relative sizes of the two beams close to the critical point. These fluctuations are artifacts of the simulation. The noise in a real system is so much weaker that the fluctuations there are probably unnoticeable. A real machine, however, should clearly exhibit the characteristic long relaxation times.

In an explicitly asymmetric collider, the two beam sizes are generally different even below the critical point (figure 13a). This condition should not be confused with a flip-flop condition which only occurs above the critical point. Note that even a conventional one-ring collider can easily be made asymmetric by running different currents in the two beam. In asymmetric systems, the more general stability condition (23) must be used.

Most machines operate below the critical point. If beam size bifurcation is a problem in a particular machine, it is sometimes possible to raise the critical point through some adjustment of the parameters  $p$ . This adjustment typically moderates the slope of the function  $S(\sigma, p)$  at the self-consistent equilibrium, thereby strengthening the stability as determined by (23). This must be done with care, however, because moderating the slope of  $S(\sigma, p)$  at equilibrium can also increase the value of  $S(\sigma, p)$ . This means that the beams are blown up more, so that the gain in luminosity achieved by higher currents could be lost to a larger beam blow-up.

The beam-size asymmetry of a typical machine operating just below the critical point is extremely sensitive to small changes in the lattice or any other of the parameters  $p$ . This is because the curves representing the functions  $S(\sigma_2, p_1)$  and  $S(\sigma_1, p_2)$  intersect almost tangentially near the critical point. Even in supposedly symmetric machines, the operators usually have to make small adjustments to balance the two beam sizes. Consequently, there is no a priori reason to believe that symmetric

machines are superior from a beam-beam point of view. It is usually assumed that maximum luminosity is achieved when the two beams are of equal size. However, even if this is true, it should be no more difficult to produce beams with equal blow-up in an asymmetric system than in a symmetric system (see figure 13b). Unequal blow-up caused by one asymmetry in  $\mathbf{p}$  can usually be eliminated by adjusting another asymmetry (for example, unequal blow-up due to different damping times might be eliminated by running each beam with different currents, with different beta functions at the IP, or different dispersions). For a more detailed discussion of this issue, see [7].

## Comments and Conclusions

The treatment described above assumes that both beams are round and that all parameters affecting the horizontal motion are identical to their counterparts affecting the vertical motion. A similar treatment can be applied to flat beams where, typically, the beam only blows up in the vertical direction. In principle, there's no reason why the assumption **B** could not be relaxed slightly and the analysis extended to more than the two variables. One might, for example, consider the horizontal and vertical widths independently. The state space would then be four dimensional  $(\sigma_{h1}, \sigma_{v1}, \sigma_{h2}, \sigma_{v2})$  rather than two  $(\sigma_1, \sigma_2)$ . The weak-strong equilibria (18) would fall on two-dimensional surfaces  $S(\sigma_h, \sigma_v; \mathbf{p})$ , and the intersections of these surfaces would be points, still corresponding to the self-consistent equilibria.

The theory of beam-beam self-consistency described in this paper is difficult to test with simulation because the assumption **B**, the one most likely to be incorrect, is built-in to most of the better known strong-strong simulation codes. It may be easier to test on a real accelerator where strong-strong beam performance can be easily compared to weak-strong. If the theory is correct, at least in its essentials, then solving the mystery of the beam-beam interaction can be reduced to understanding weak-strong blow-up, and specifically, to understanding the shape and parametric dependencies of the weak beam size function  $S(\sigma; \mathbf{p})$ .

This work was funded by DOE and performed at the Lawrence Berkeley Laboratory under contract DE-AC03-76SF00098. I am grateful to the Exploratory Studies and Collider Physics groups at LBL for their generous support.

## References

- [1] A.B. Tyomnikh, "A Phenomenological Model of the Flip-Flop Effect in Colliding Beams", INP preprint 82-148 (1982). (in Russian)
- [2] K. Hirata, Phys. Rev. Letters **58**, No.1, p. 25 (1987)
- [3] M.A. Furman, K.Y. Ng, A.W. Chao, "A Symplectic Model of Coherent Beam-Beam Quadrupole

Modes", SSC preprint 174 (1988).

- [4] M. H. Donald and J. M. Paterson, "An Investigation of the 'Flip-Flop' Beam-Beam Effect in SPEAR", IEEE Trans. Nucl. Sci. , NS-26, No. 3, 3580 (1979).
- [5] R. Littauer, "Multibunch Operation of CESR", IEEE Trans. Nuc. Sci. NS-32, No. 5, 1610 (1985).
- [6] Such a diagram implies the extension of assumption **B** to the entire phase plane.
- [7] J. L. Tennyson, " Beam-Beam Effects in an Asymmetric Collider", In preparation.

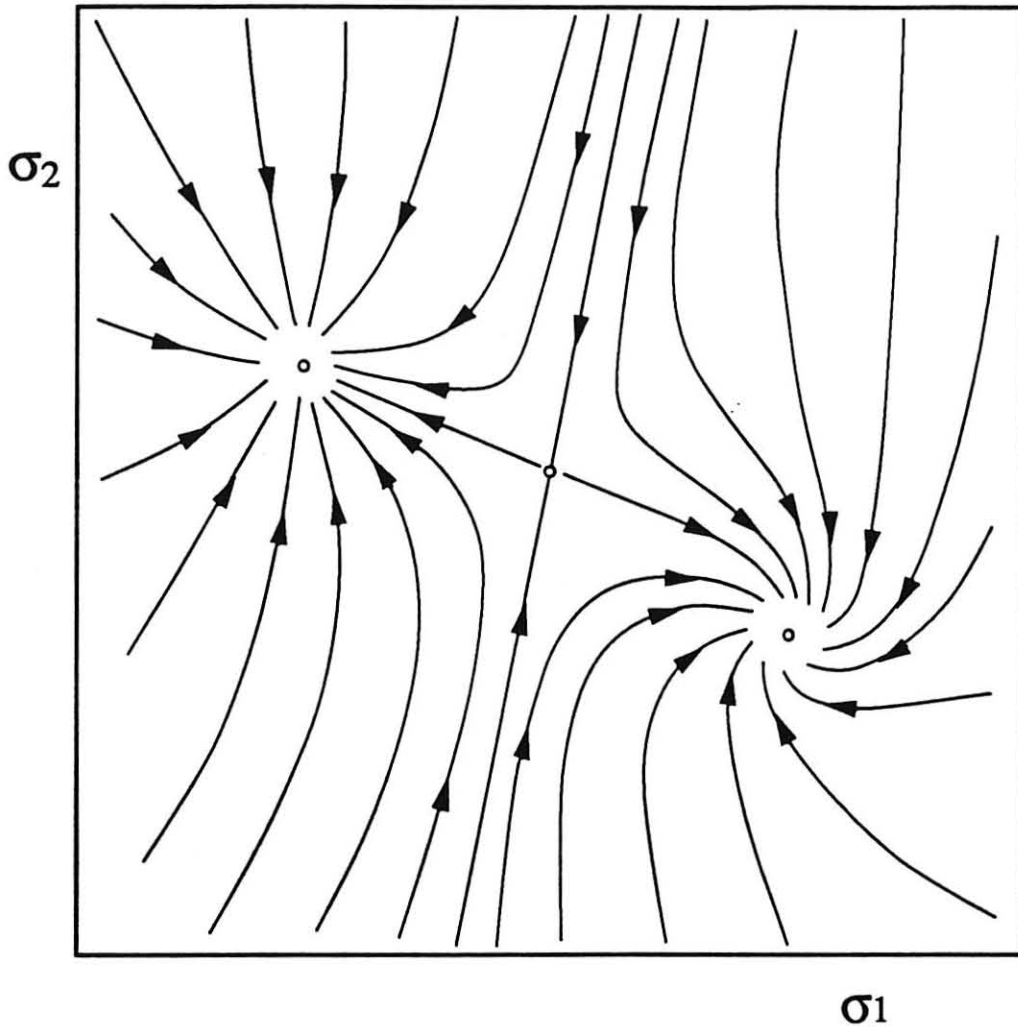


Figure 1. A vector field in the  $(\sigma_1, \sigma_2)$  plane. The flow lines shown here lie parallel to the vectors and represent trajectories of the beam system as it approaches equilibrium. This field exhibits three equilibria: from left to right, a stable node, an unstable saddle, and a stable focus. The two basins are separated by a boundary that intersects the saddle point.

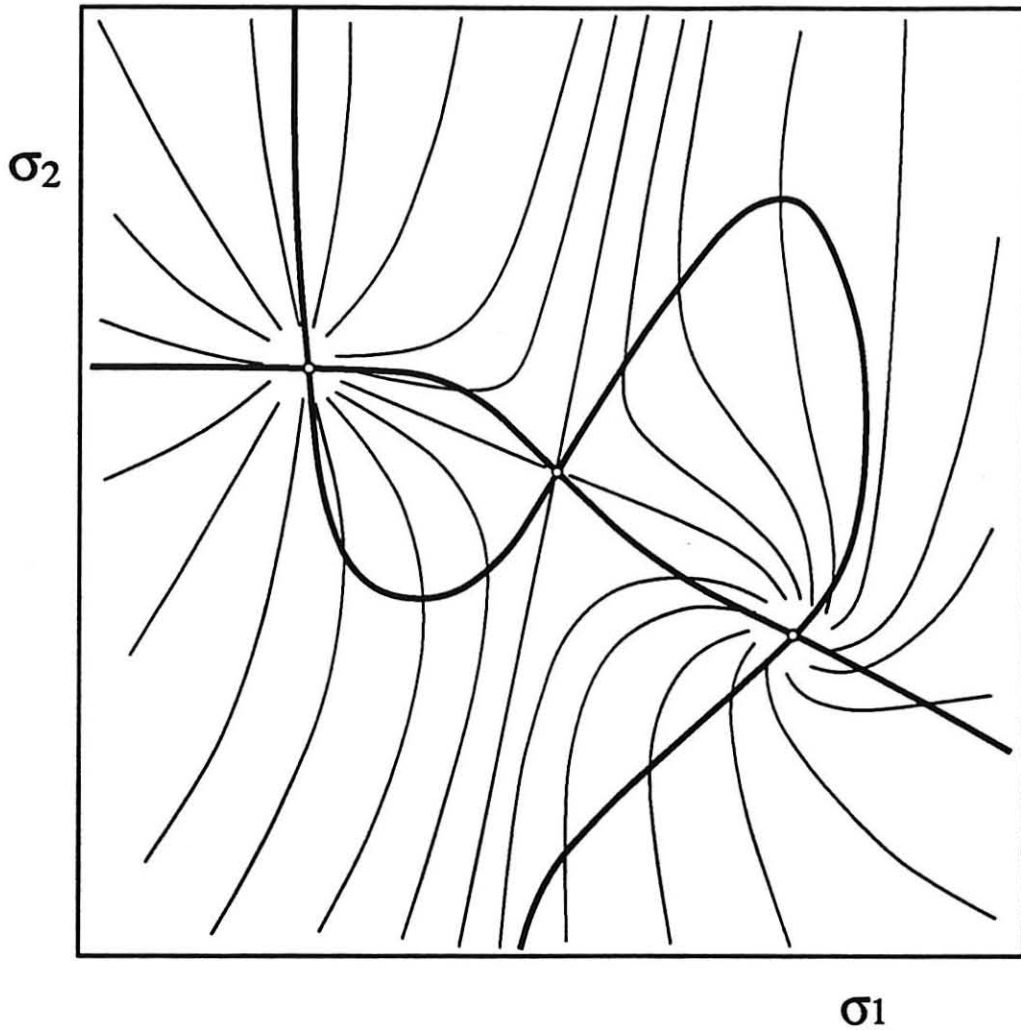


Figure 2. The curves corresponding to  $\dot{\sigma}_1 = \dot{\sigma}_2 = 0$  are superimposed on the vector field shown in figure 1. These curves correspond to points where the flow lines are either vertical or horizontal. The intersections of these curves correspond to the self-consistent equilibria.

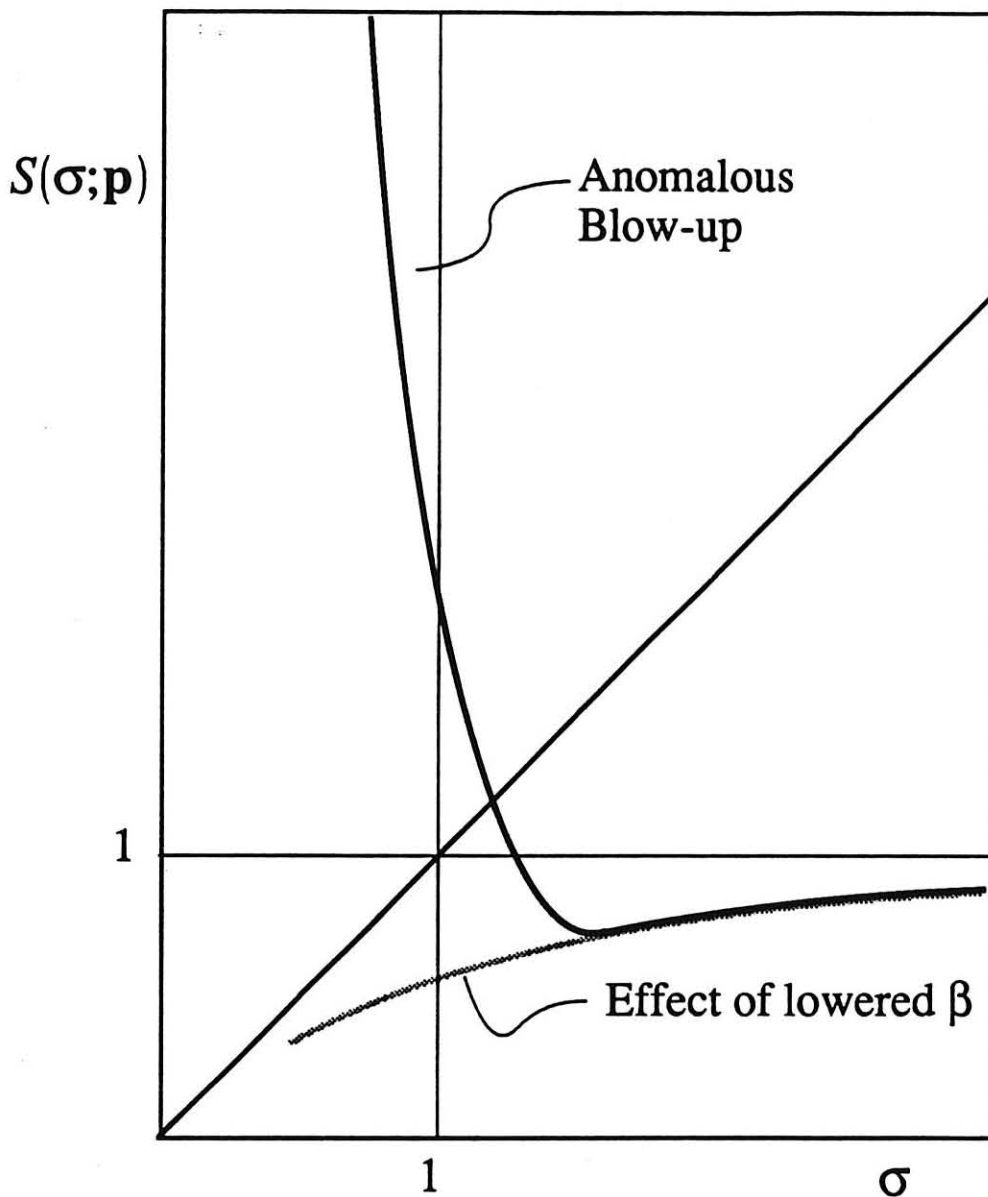


Figure 3a. A schematic representation of the weak beam size function for fractional tunes  $0 < \nu < .25$ . Tunes in this range, together with the linear focusing of the beam-beam force, reduce the beta function, and thus the beam width, at the IP. As  $\sigma$  decreases, the beam shrinks until the linear tune shift  $\xi$  reaches a certain threshold. Below this threshold, the weak beam blows up due to incoherent beam-beam effects.

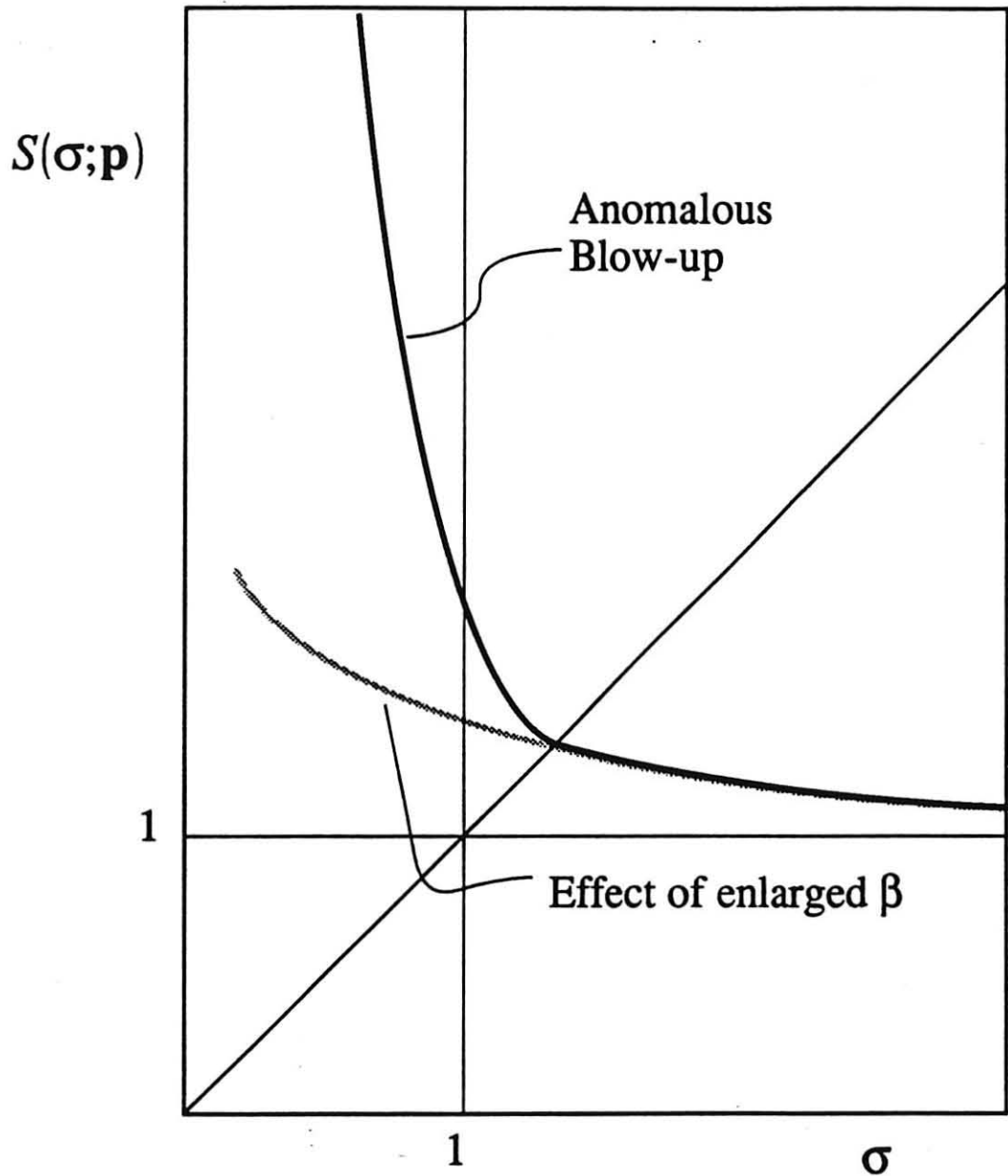


Figure 3b. Similar to fig. 3a, but here the tunes of the weak beam are  $.25 < \nu < .5$ . The focusing action of the beam-beam interaction now results in a small increase in the beta function and a corresponding expansion at intermediate values of  $\sigma$ .

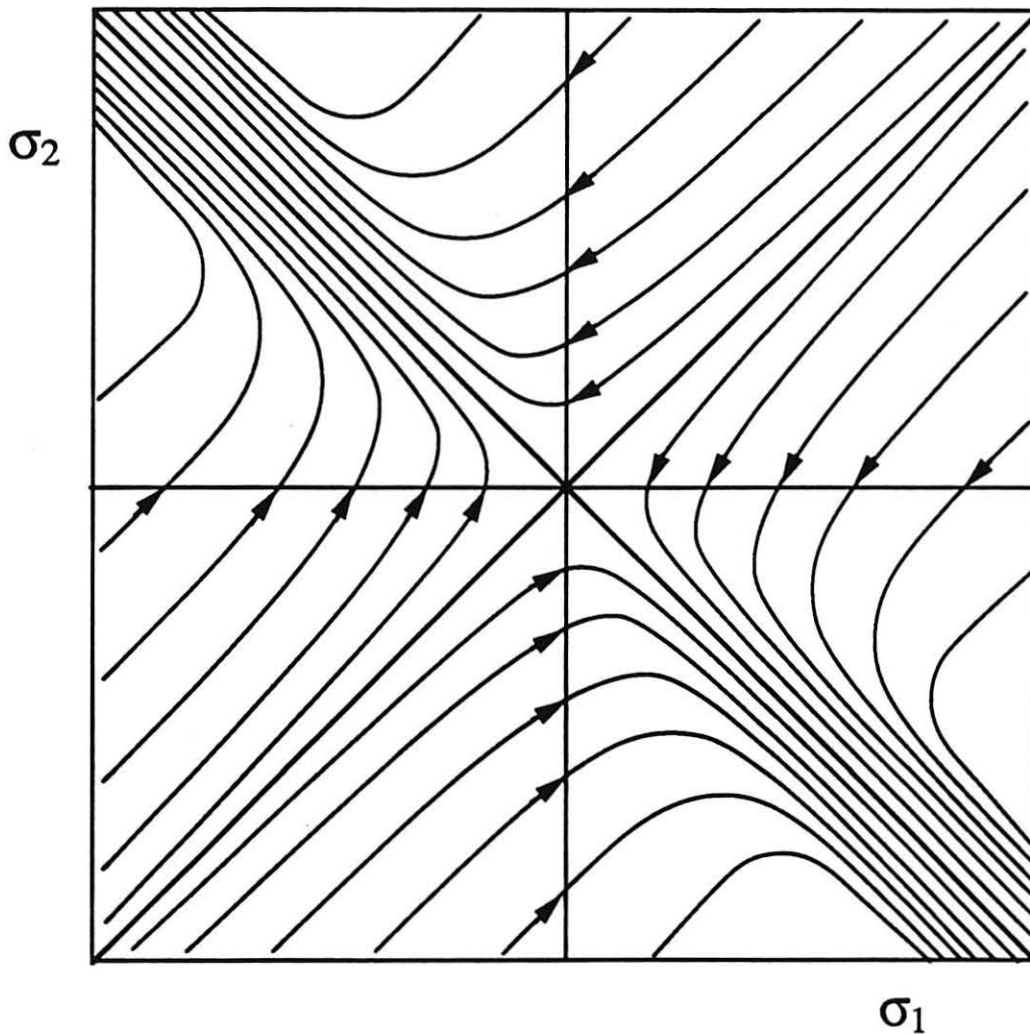
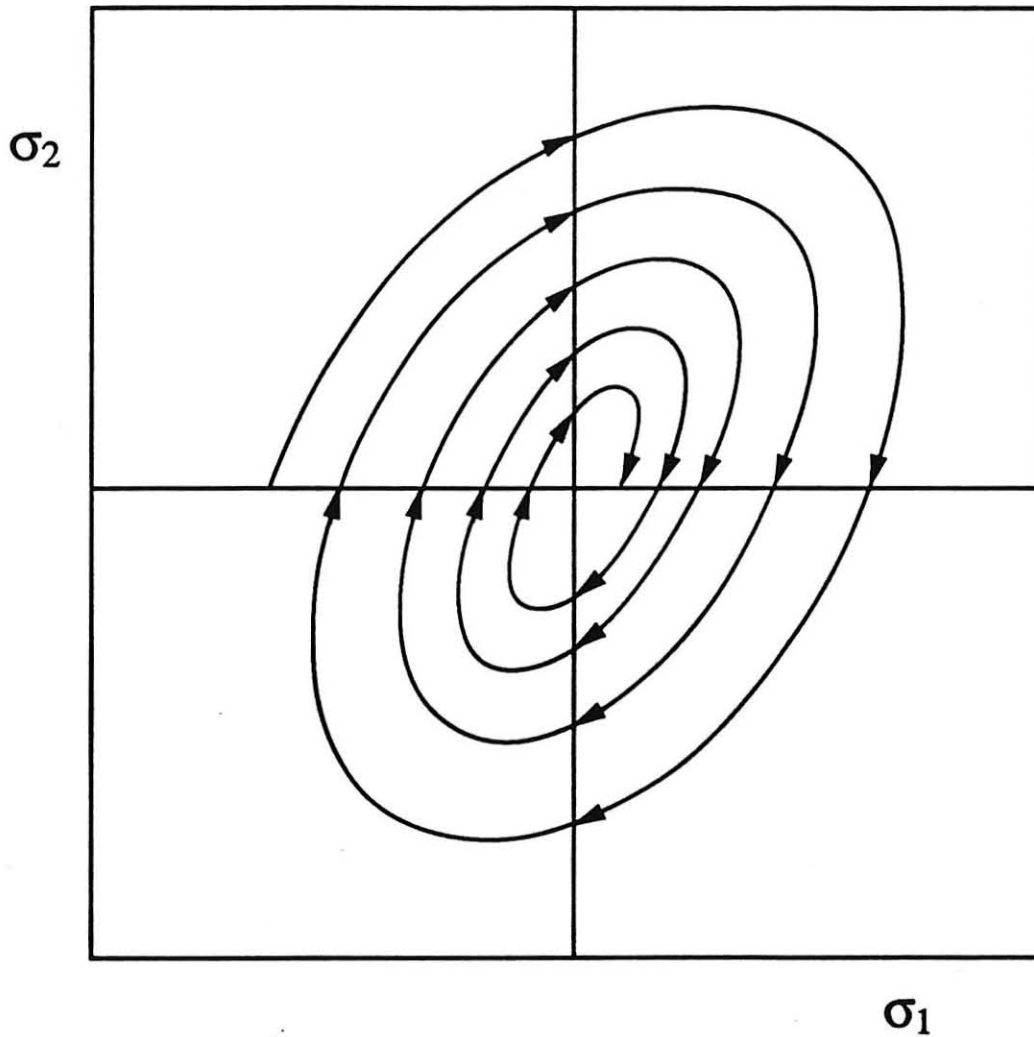


Figure 4a. Phase flow in the vicinity of a saddle point for which both weak-strong equilibria are stable. When the motion is constrained to either the horizontal or vertical intercept, it is stable (all arrows point inward).



**Figure 4b.** Phase flow in the vicinity of a stable focus for which one weak-strong equilibrium ( $\sigma_{eq2}$ ) is unstable. Motion constrained to the vertical intercept moves away from the equilibrium.

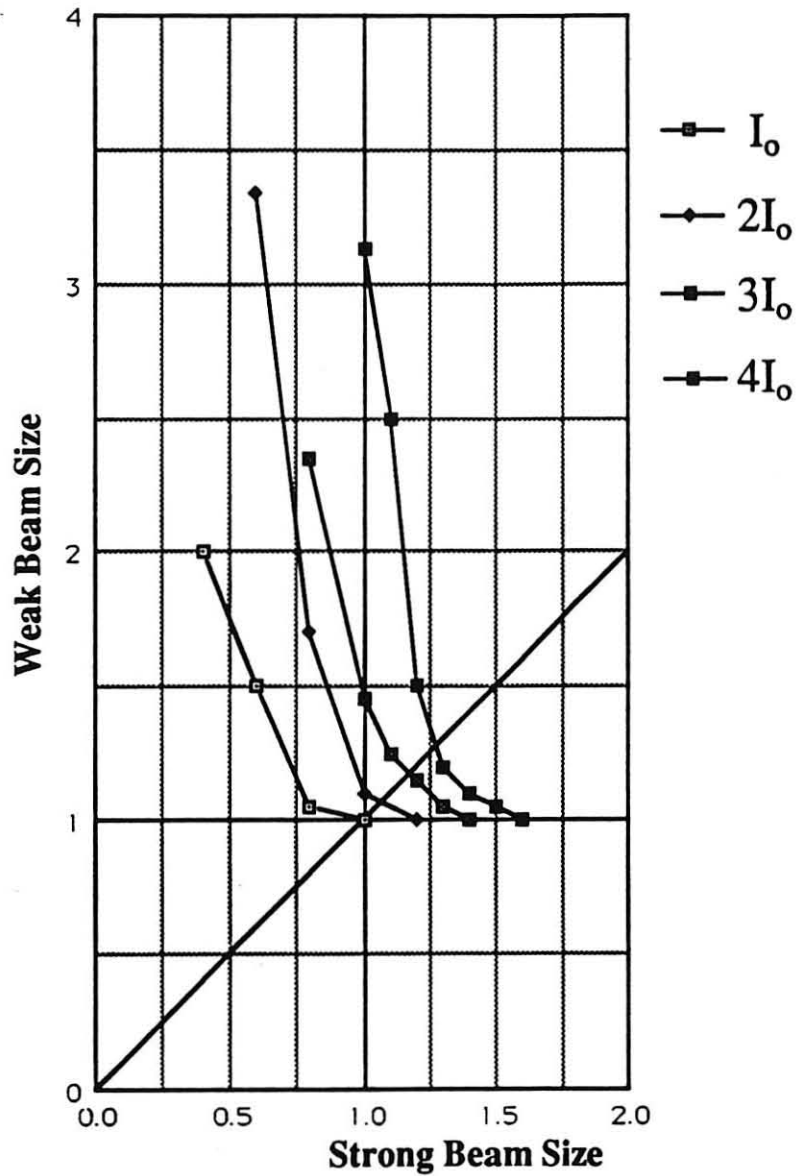


Figure 5. Weak beam size function  $S(\sigma;p)$  for four different values of the strong beam current. These curves are derived from weak-strong simulation. The bifurcation will occur at  $3I_0$  since this is where the slope of  $S(\sigma;p)$  is -1 on the diagonal.

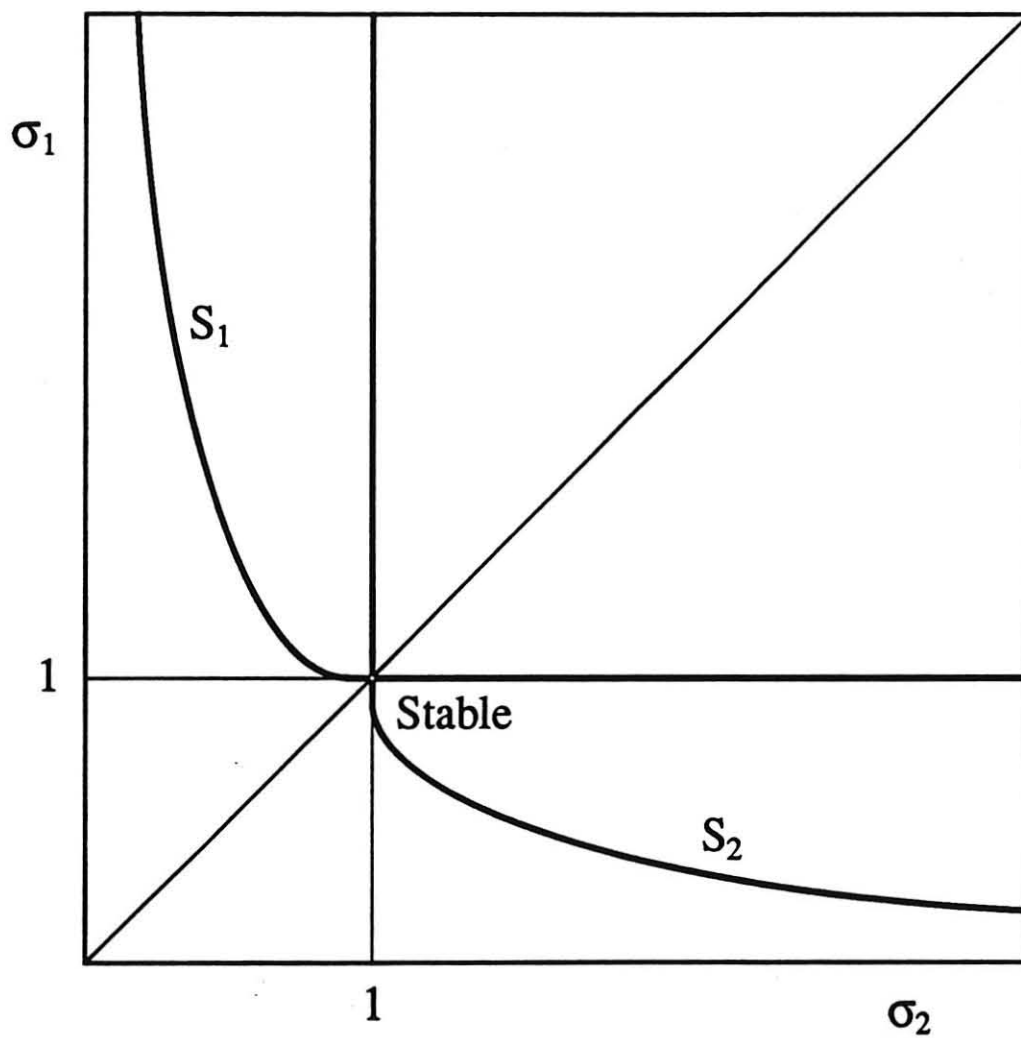


Figure 6. Stable equilibrium at low currents and with no blow-up. The two beams are symmetrical.

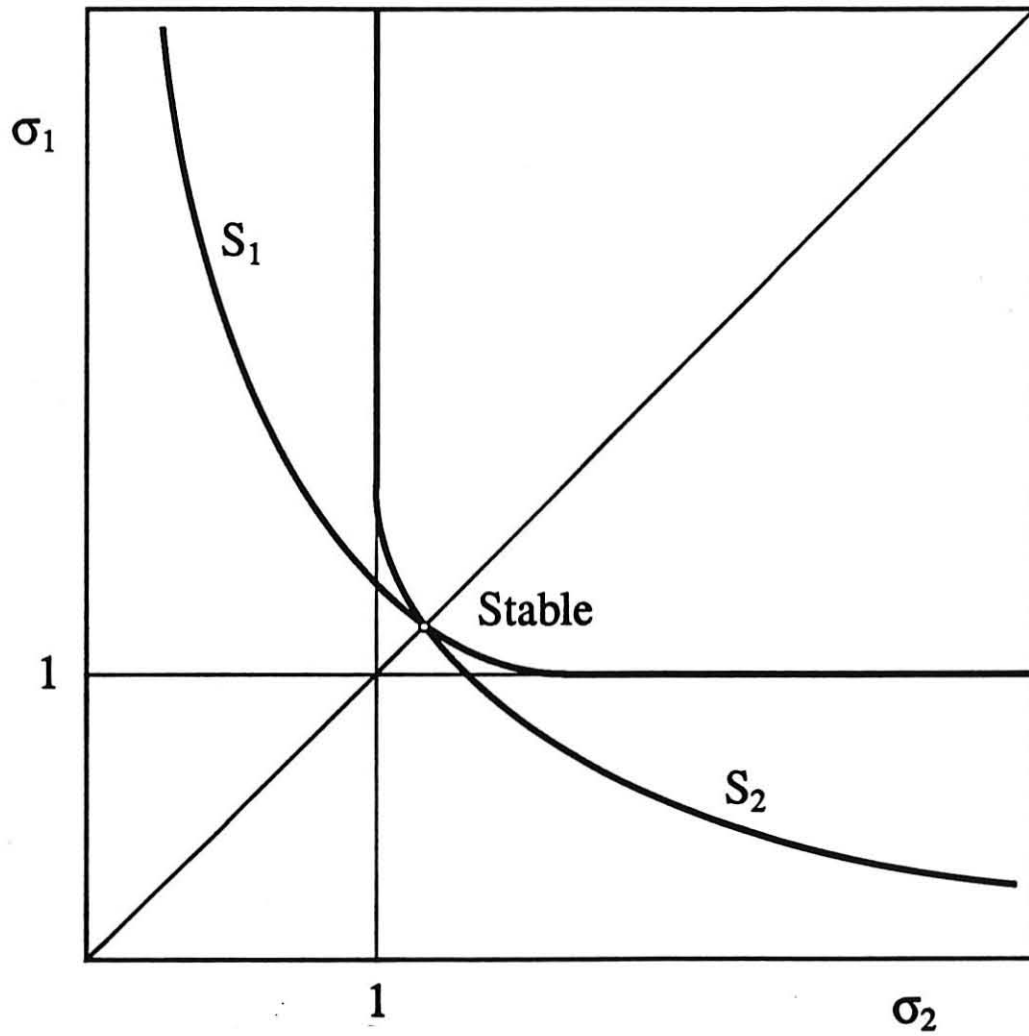


Figure 7. Stable equilibrium at moderate currents for symmetric beams. Both beams are slightly blown up.

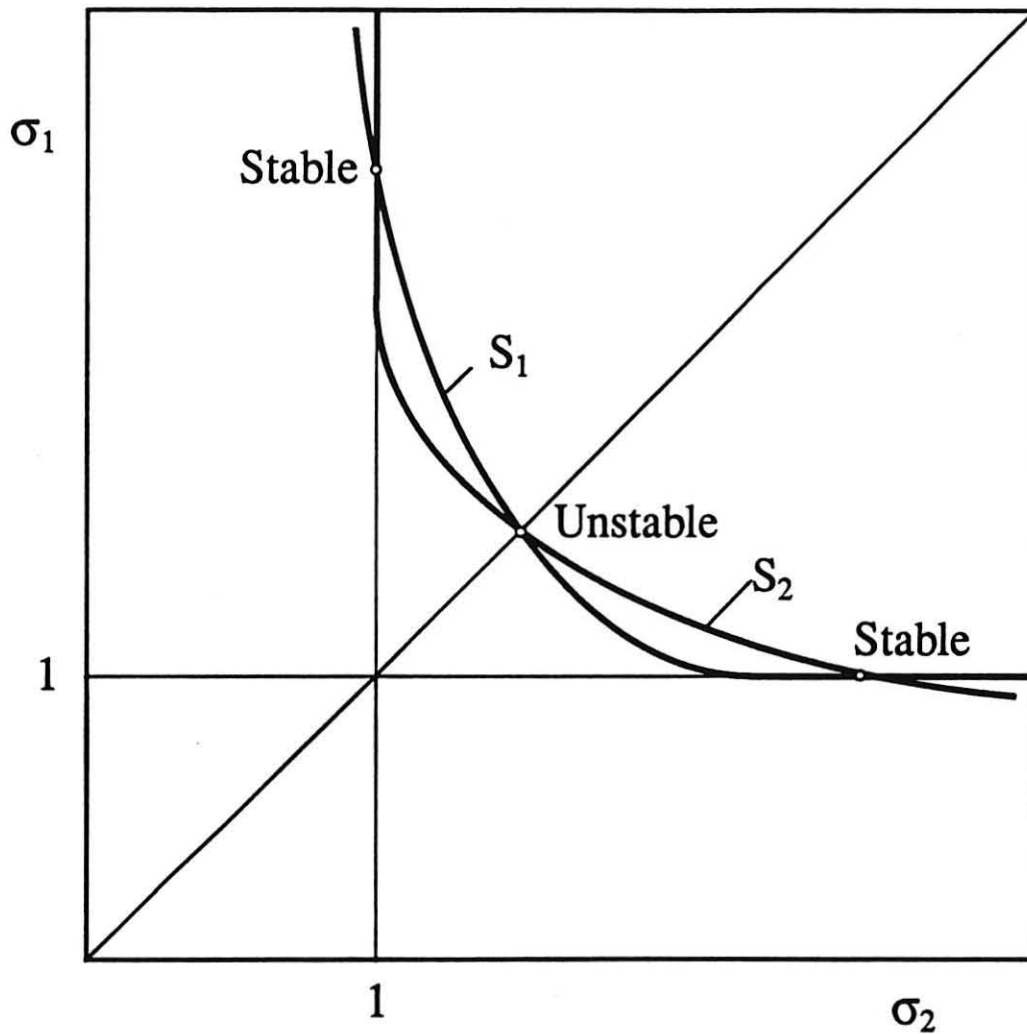


Figure 8. The beam system above the critical point. There are now three equilibria. Although the system is still symmetric, the two stable equilibria correspond to asymmetric flip-flop states.

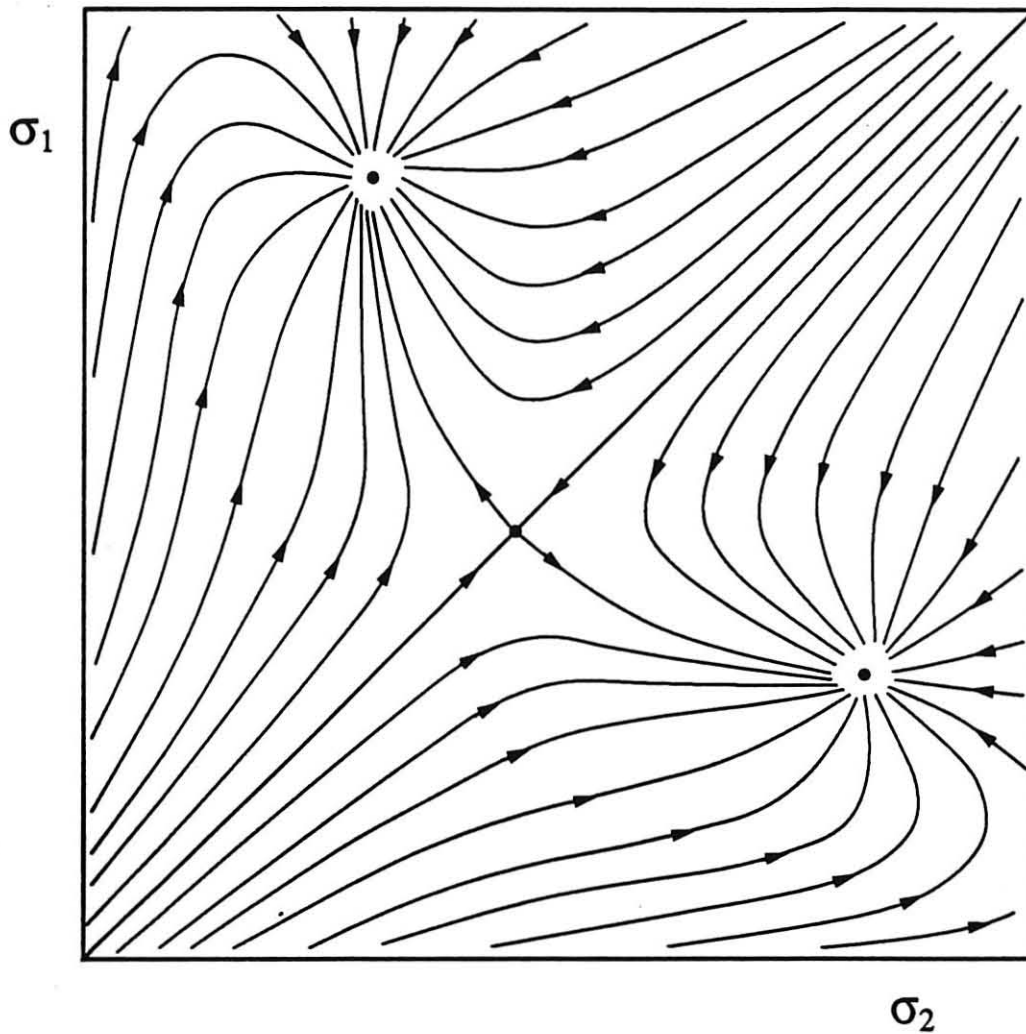


Figure 9. Typical phase flow for the symmetrical beam system above the critical point. This flow corresponds approximately to the weak beam size functions shown in figure 8.

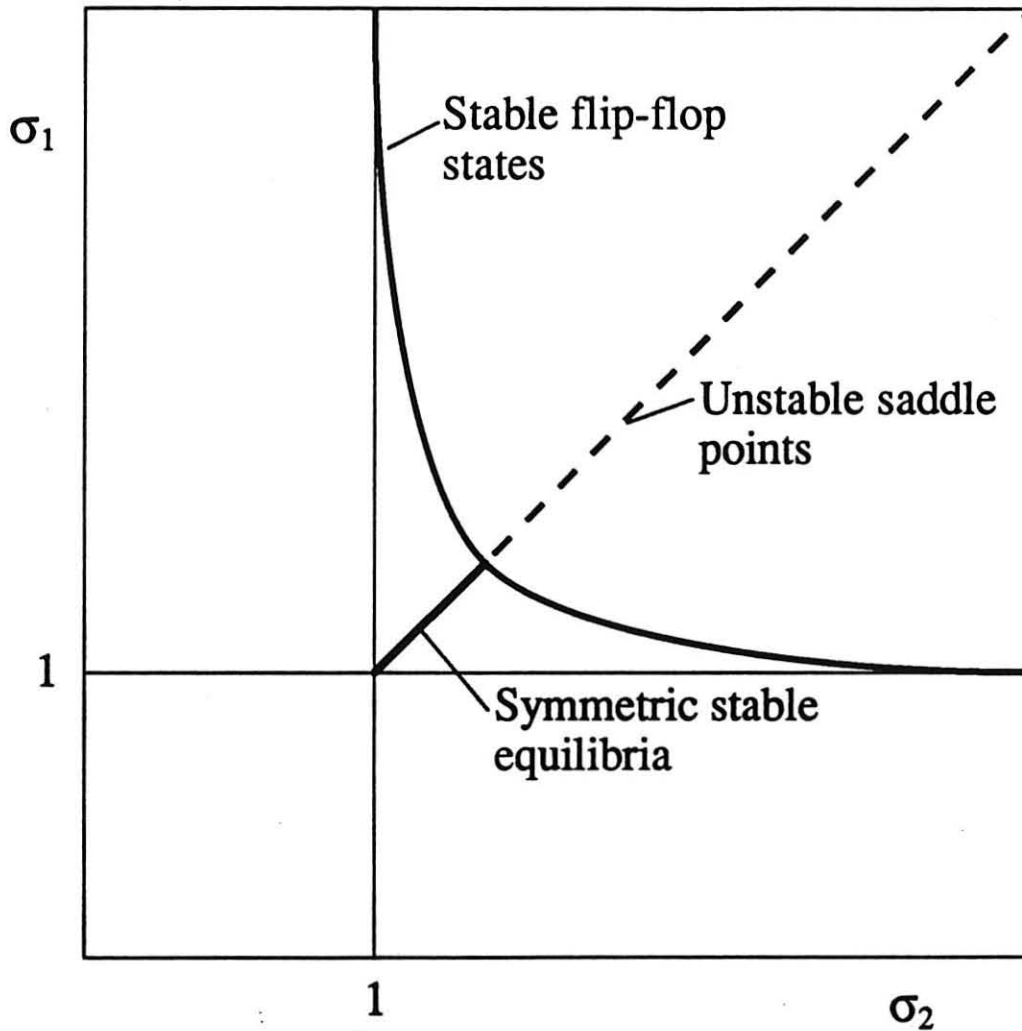


Figure 10. Curves of stable (solid) and unstable (dashed) equilibria for a range of current values. These curves follow the intersections of the two functions  $S_1$  and  $S_2$  as the current is increased. The currents in the two beams are constrained to be equal.

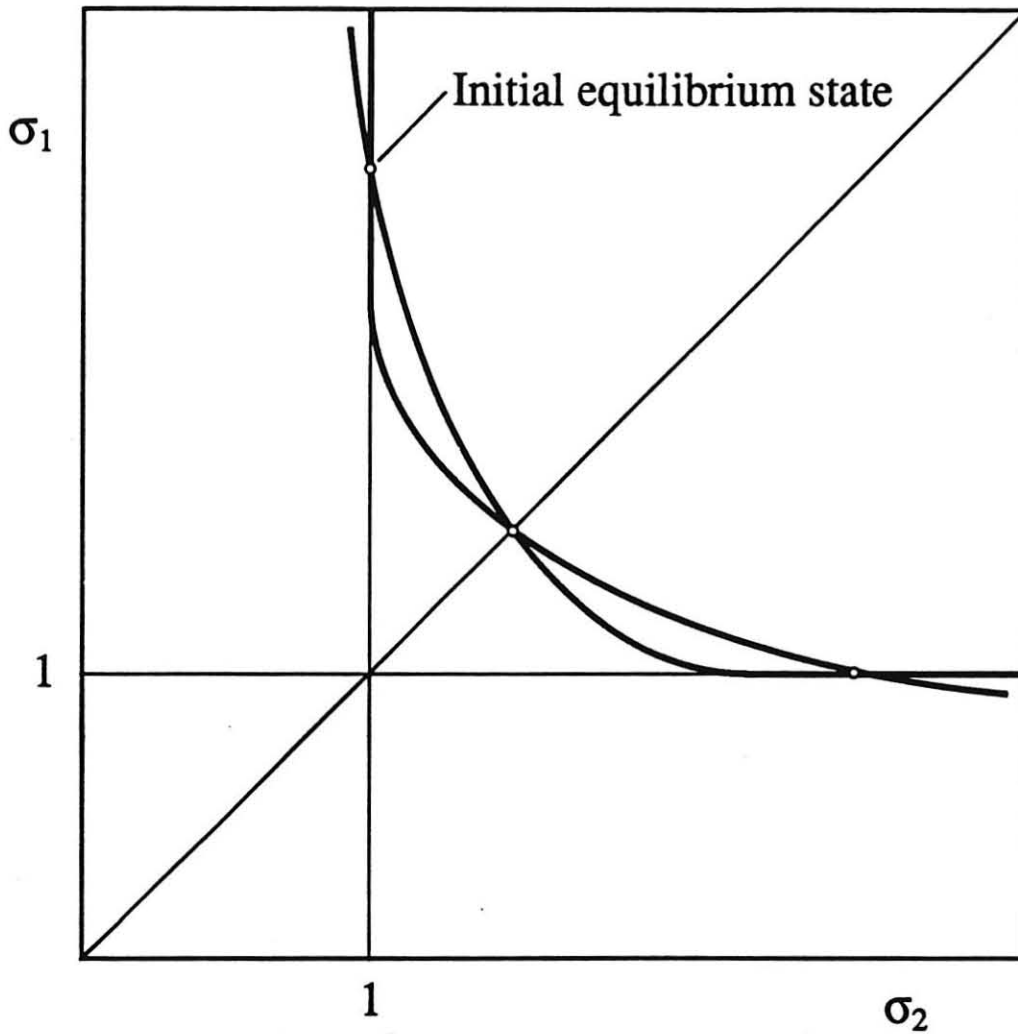


Figure 11a. The system is initially symmetric but above the critical point. It is in an asymmetric flip-flop state, with beam #1 blown up and beam #2 close to its unperturbed size.

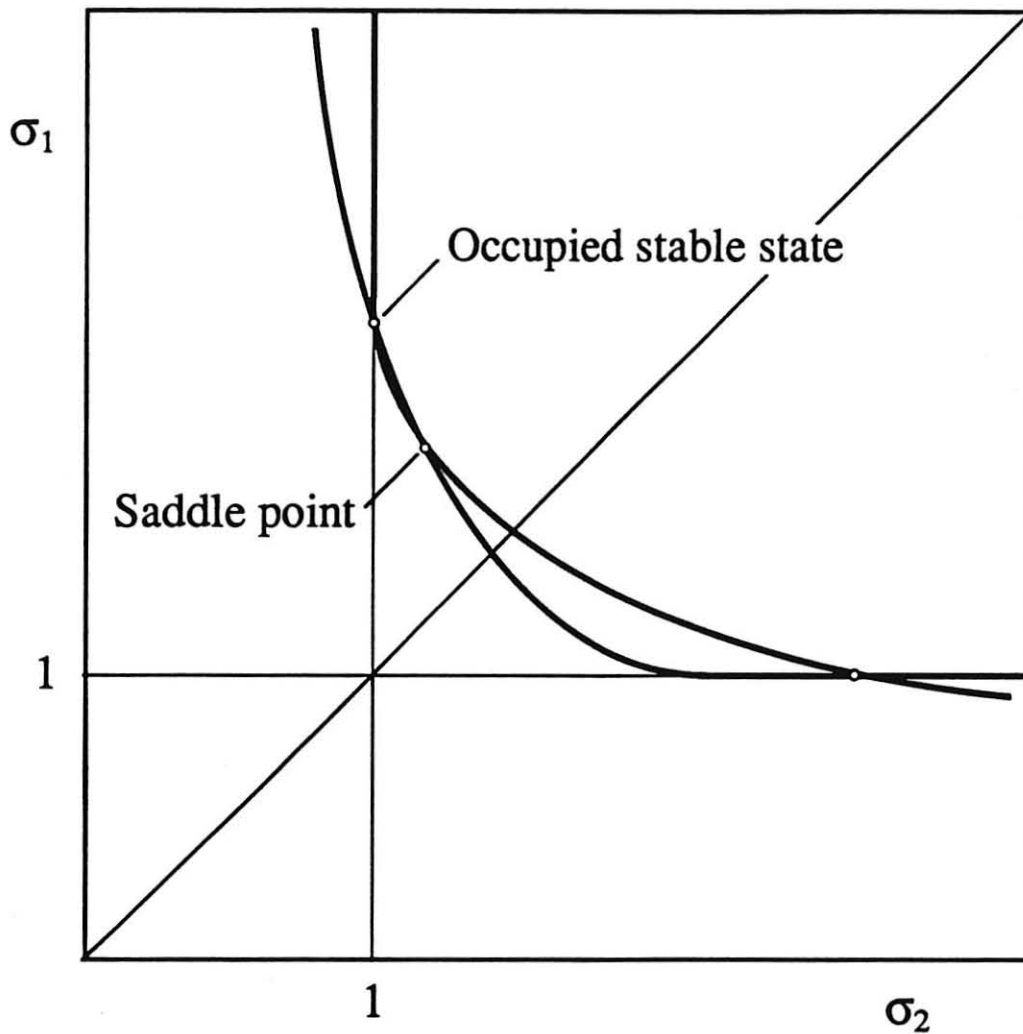


Figure 11b. As the current in beam #2 is decreased, the graph of  $S_1$  moves to the left. The occupied stable equilibrium and the saddle point equilibrium approach one another. The size of beam #1 decreases slightly.

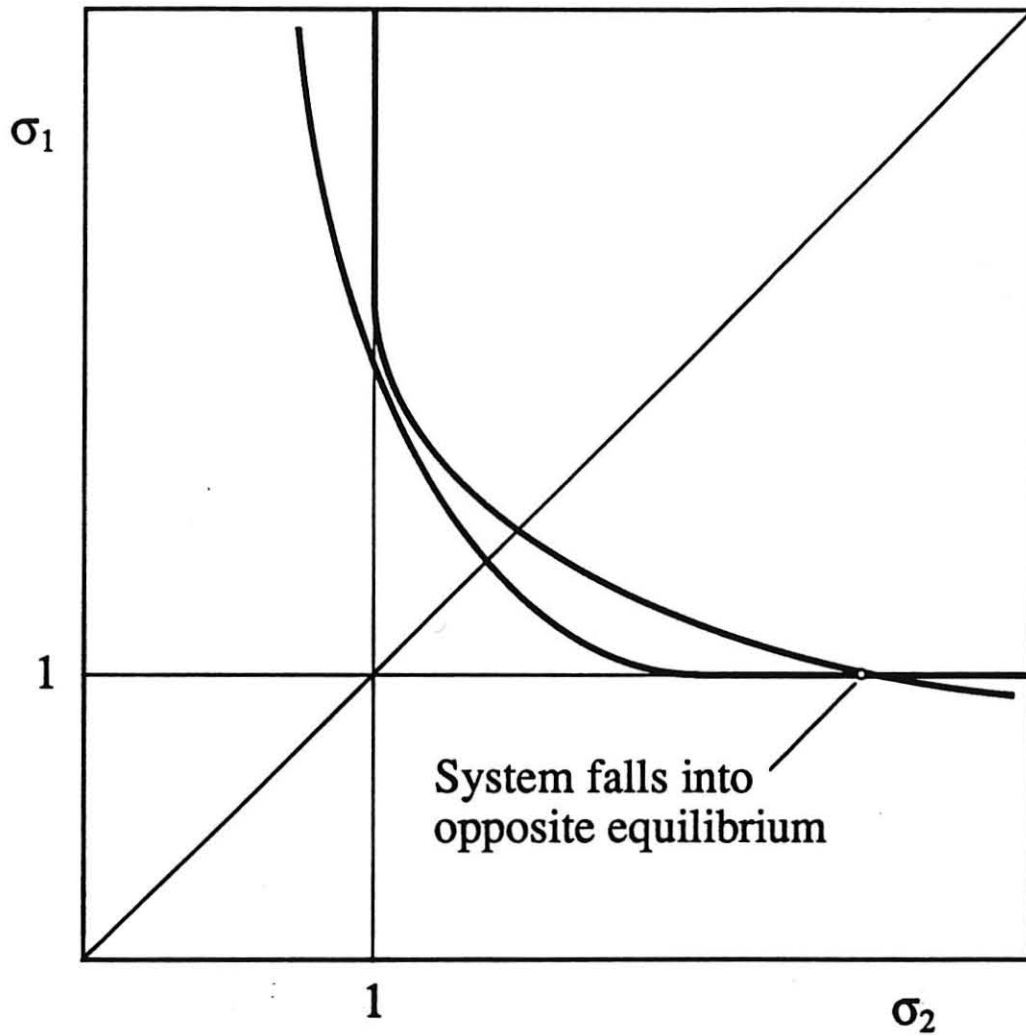


Figure 11c. As the current in beam #2 decreases further, the stable equilibrium and saddle point meet and then disappear. The system "flips" into the opposite flip-flop state.

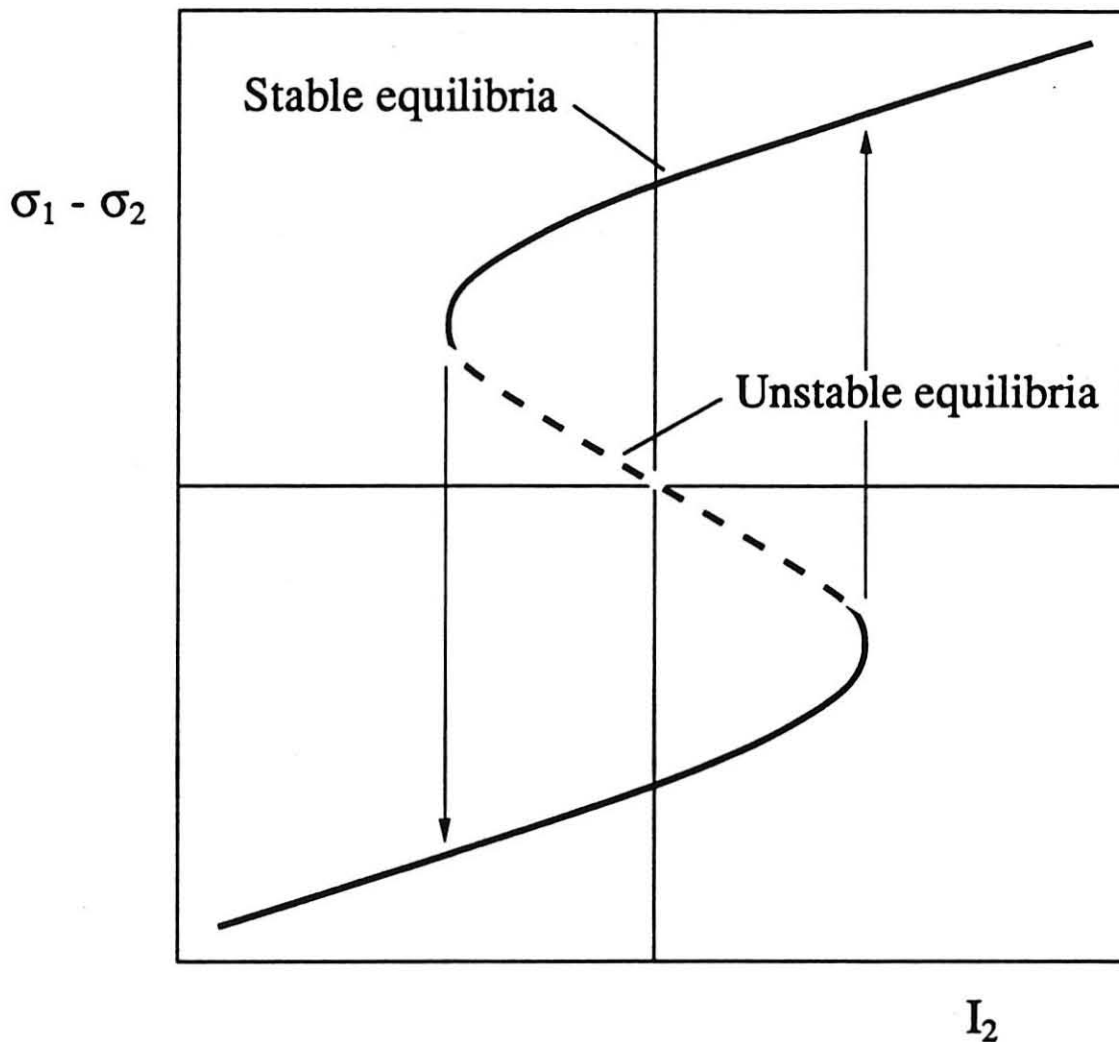


Figure 12. Hysteresis curve for the beam flip illustrated in figure 11. This is a typical "cusp catastrophe". The system falls off the fold when the current in beam #2 is varied.

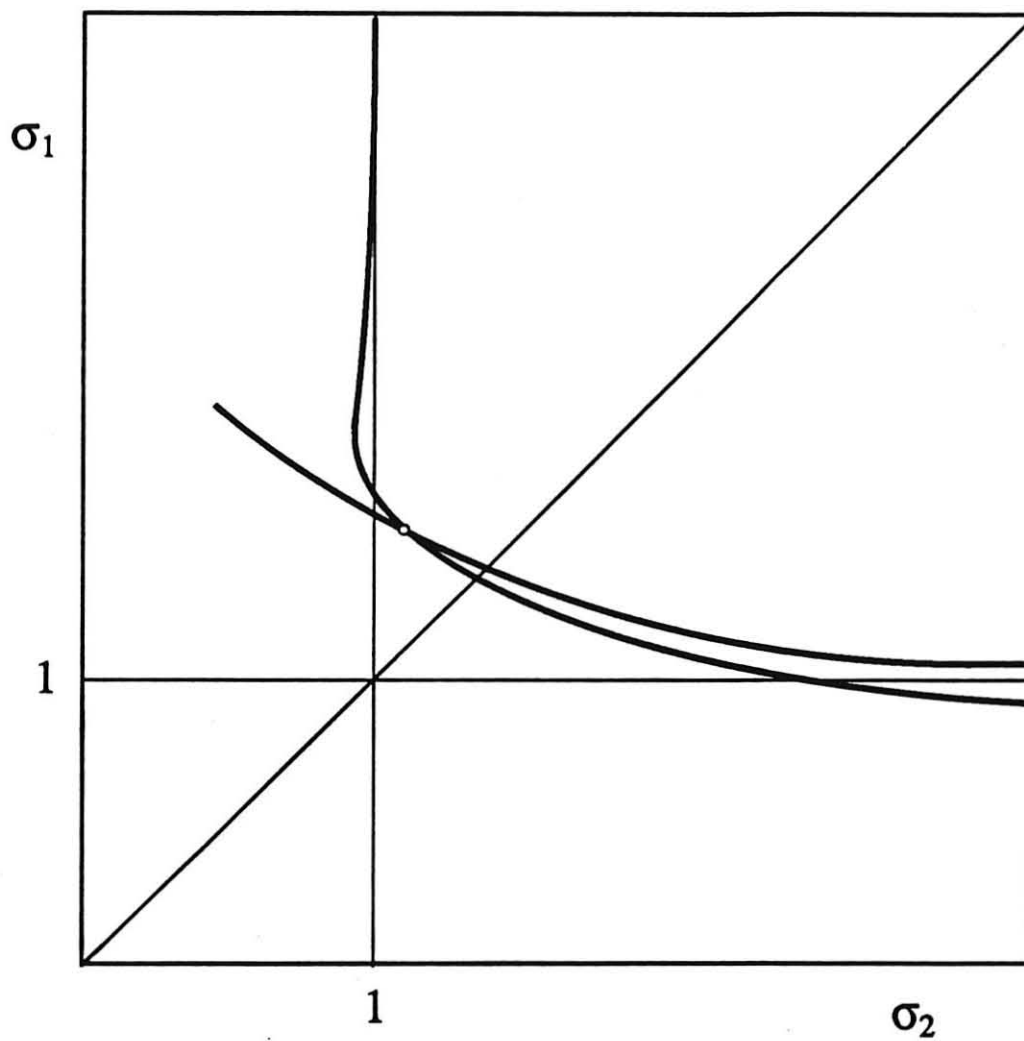


Figure 13a. An asymmetric system below criticality. There is one stable, asymmetric equilibrium. This is not a "flip-flop" equilibrium.

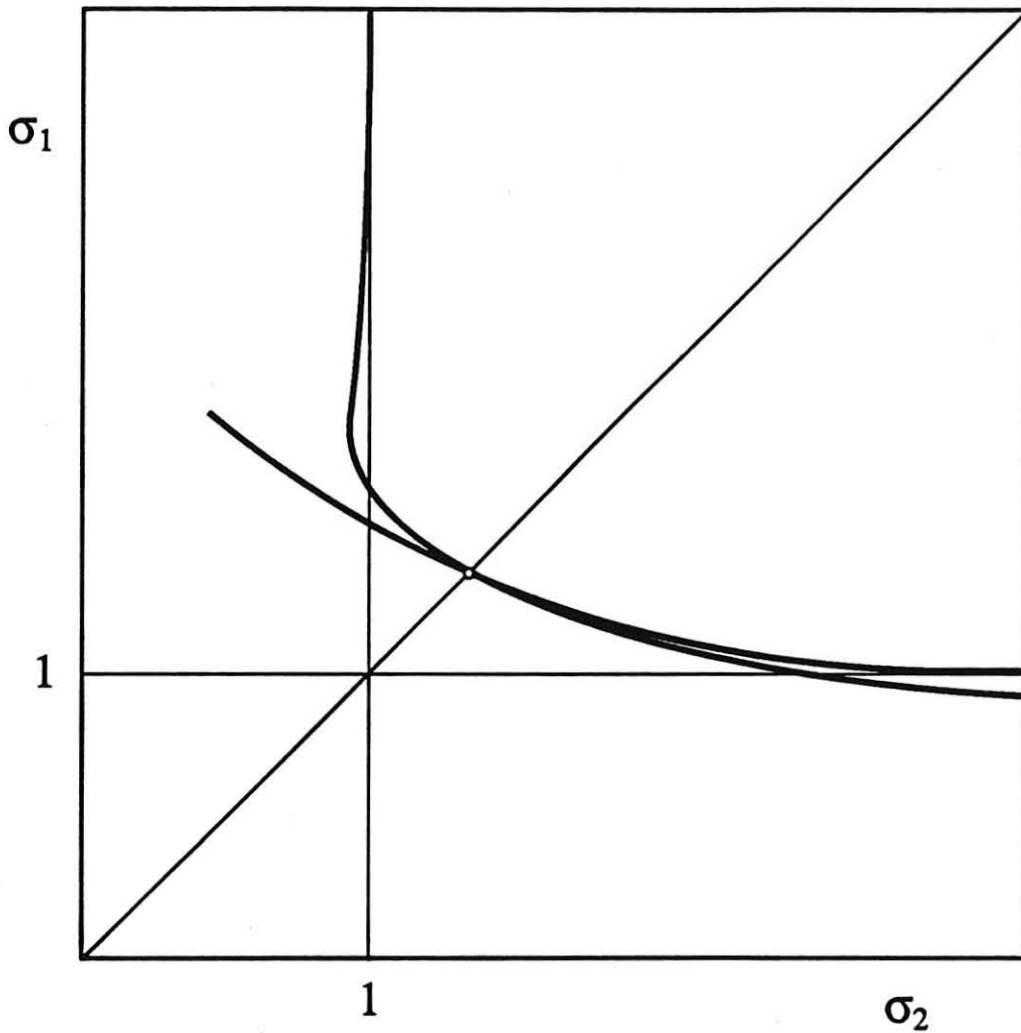


Figure 13b. Another asymmetric system below criticality. As before, there is a single stable equilibrium. Here, however, the parameters  $p$  have been fined-tuned to make the equilibrium symmetric.